KnE Materials Science

ASRTU Conference Proceedings
IV Sino-Russian ASRTU Symposium on Advanced Materials and Processing Technology (2016), Volume 2016

Knowledge E
Engaging minds

Conference Paper

Forecasting Durability and Cyclic Strength of Aluminum Alloy AA2219 Using Fractal Analysis of Acoustic Emission

O.E. Sysoev, D.G. Kolykhalov, E.A. Kuznetsov, and S.V. Belykh

Komsomolsk-na-Amure State Technical University, 681013 Komsomolsk-on-Amur, Russia

Abstract

Acoustic emission (AE) monitoring was used to examine the fatigue failure of aluminum alloy AA2219 under cyclic loading. AE fractal analysis revealed separate sources of elastic waves on the macro-, meso-, and micro-levels of the deformed material. The correlation between the number of AE hits, revealed during the first loading cycle, from the AE sources was shown on the macrolevel and the number of loading cycles, leading to the destruction of the sample. Results achieved allow forecasting durability of materials made of AA2219 alloy right after the first loading half-cycle.

Keywords: acoustic emission, fractal analysis, cyclic loading, forecasting, durability, cyclic strength

Corresponding Author: S.V. Belykh; email: Belykhsv@knastu.ru

Received: 9 September 2016
Accepted: 19 September 2016
Published: 12 October 2016

Publishing services provided by Knowledge E

Selection and Peer-review under the responsibility of the ASRTU Conference Committee.

OPEN ACCESS

1. Introduction

Test low-cycle loading with conditions, not leading to the strength reduction of structures and components but allowing investigation of sample behavior under loading, is a promising method of determining the durability of structures and components. Acoustic emission (AE) method is efficient means of analyzing physical processes taking place in the material during test loading [1, 2].

Multiple studies testify that AE is observed in the elastic strains field under the strain in the range from 0 to σ_T [3-5]. Its presence is related to the formation of submicrocrack and the brittle fracture of the dispersions. In many cases, AE generated as a result of elastic strain is also determined by the second phase cracking. The number of various inclusions in steel alloys (carbides, silicates, sulphides, etc.) is 10^9–10^{12} per kg, and the possibility of their destruction should not be ignored even in case of loading in the elastic field [6].

The major AE sources being a result of loading in the low-elastic field are either formation of imperfections or plastic strains occurring in separate micro-volumes of the material [4]. In case of local plastic strain, AE sources are movements of single dislocations and their clusters, their separation from the pinning points, Frank-Read dislocation source response, annihilation of dislocations, and their yield to the free surface.

Acoustic emission source	AE momentum energy	AE source scale
Frank-Read dislocation source	10^{-21} J	micro
Single dislocation movement	10^{-23} J	
Group movement of *n* dislocations	$n \cdot 10^{-23}$ J	
Separation of a single dislocation from the pinning point, dislocation hindering by the obstacle	10^{-19} J	meso 1
Separation of a group of *n* dislocations from the pinning point, hindering of a group of dislocations by the obstacle	$n \cdot 10^{-19}$ J	
Annihilation of the dislocations at the free surface or grain boundaries	$2 \cdot 10^{-18}$ J	meso 2
Microcrack formation	10^{-10}–10^{-12} J	macro
Second phase cracking	10^{-11}–10^{-12} J	

Table 1: Parameters of AE signals for separate sources of acoustic emission [7, 8].

From the analysis point of view, it is convenient to divide AE sources into several scale levels: micro-, meso- and macrosources, according to their radiation energy E (Table 1).

Apparently, the radiative energy scale of the AE source is related to its linear dimensions. Thus, AE macrosources are macroobjects with dimensions comparable to the dimensions of the analyzed sample, second level mesosources are acting in the scale of the material's grains, first level mesosources have the dimension scale of dislocation condensation (condensation of dislocation structures), and microsources have linear dimensions of the same scale as that of lattice interatomic spacing.

The sensitivity threshold of the modern equipment to record AE is 10^{-17} J, so the confident AE recording caused by the material loading requires at least 10^6 dislocations in motion, 10^4 Frank-Read sources activated, no less than 10^2 dislocations separated from the pinning point and no less than 5 dislocations reached the grain boundary. There are 10^6 microsources or 100 mesosources of the first level or 5 mesosources of the second level or 1 macrosource simultaneously taking part in formation of each AE hit recorded by equipment. One can judge of the dimensional scale of the sources and of the process nature, leading to the AE event. The number of sources to form AE hit can be found by non-linear dynamics methods [9, 10]. If each hit is viewed as a time sequence, caused by the dynamic system, then revealing the number of AE hit sources is reduced to determining degrees of freedom of this dynamic system in the one-dimensional projection of its evolutions in the phase space.

Methods of non-linear dynamics allow reconstructing the multidimensional attractor from one-dimension time sequence. Metrical properties of the multidimensional attractor are very close to the evolutions of the dynamical system analyzed [11, 12]. That said, phase space dimension of the analyzed process and the number of its degrees of freedom can be determined with a high level of accuracy.

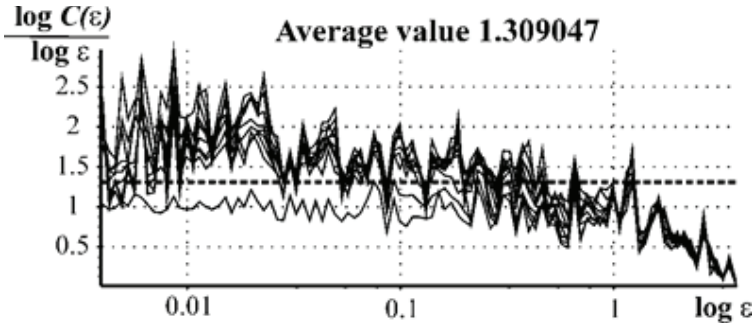

Figure 1: Calculating of the fractal dimension D_2 on Rapp's plots with the help of *TISEAN* software. For the given signal $D_2 \approx 1.309$.

2. Methods

Testing machine MI-40KU [13] was used to analyze the possibility of predicting the cyclic strength according to the characteristics of the recorded AE signals. The machine generates force up to 40 kN and allows testing the samples on extension, compression, and spinning. Load force setting accuracy is ±10 N, the inaccuracy of linear strain measurements does not exceed 1 μm and that of angular strain ones does not exceed 0.05 degrees. Acoustic emission signal recording was executed with the help of Adlink PCI-9812, a 12-bit analogue-digital card. The signal has been recorded by AE detector, attached to the sample. ADC sample rate was 20 MHz, oscilloscope record length was N = 16384 samples. A standard tubular sample was used for testing. The detector was placed to the polished flat surface of the sample. The acoustic joint between the detector and the sample was filled with silicone fluid.

Fractal characteristics of the AE signal and the attractor, which was reconstructed by the AE signal pattern, were calculated with the help of *TISEAN 3.0.1* software [14-16]. The correlation dimension was calculated as follows. Firstly, correlation totals were calculated by *d2.exe* software. Input data were set to be within [0,1] interval, with the variable lag τ set. Since it is quite challenging to determine the longest linear segment of local bending on the Rapp's graph [16], D_2 was calculated as an average value of the graph [17] (Fig. 1).

Since the analyzed dynamic system has many degrees of freedom, the dimension $D_{emb.}$ of the lag space for the attractor reconstruction was taken equal to 512. Values of correlation dimension $D_2(\tau)$ for the variable lag were calculated for this phase space. The variable lag took on values τ_i = 1, 2, ⋯, τ_{max}, where $\tau_{max} = N/D_{emb,} = 32$. The maximum of $D_{2attr.}(\tau_i)$ values obtained was perceived as the fractal dimension of the reconstructed attractor $D_{2attr.}$.

3. Results

The testing process included 4-15 loading cycles and ended with the complete destruction of the sample. Load force F was changed according to a sinusoidal pattern from 0 to 20 kN. Fig. 2 features graphs of correlations observed for the sample, which was

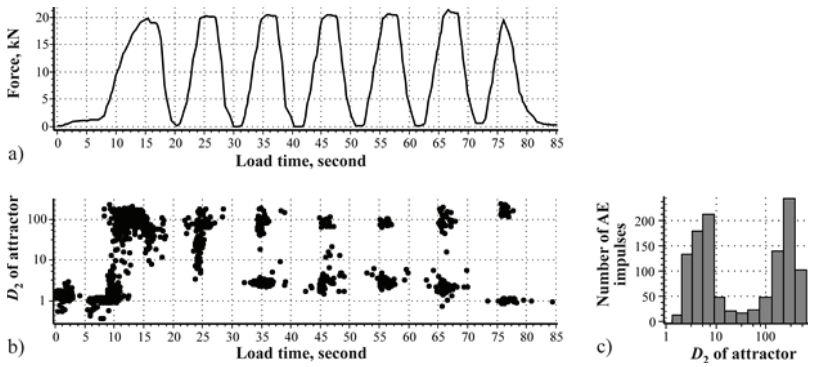

Figure 2: Correlations, observed during the cycle loading of the sample from AA2219 alloy: *a* load force; *b*, *c* fractal dimension $D_{2attr.}$ of the attractors, reconstructed based on oscillograms.

destructed after 7 loading cycles. From 1 100 to 2 600 AE hits were recorded during the testing.

Analysis of AE signals was aimed at evaluating the scale of the processes, leading to separate recorded hits. An attractor was reconstructed and its fractal dimension $D_{2attr.}$ was calculated for each AE signal (Fig. 2c,d). According to theory [12], the attractor's parameters ($D_{emb.}$ = 512, $\tau = 1, \cdots, 32$) allow evaluating the number *m* of degrees of freedom for processes, leading to the AE hit in the range from 1 to ($D_{emb.} - 1$) / 2 = 255. Let us attribute AE sources with *m* = 1 ÷ 6 (attractor's fractal dimension $1 \leq D_{2attr.} \leq 6$) to macroscale and associate them with macrodefects of the material and the inclusion of second phases.

Signal sources with the attractor reconstruction value of $6 < D_{2attr.} \leq 25$ (*m* = 7÷25) will be considered as resolution of *m* dislocations to the surface (mesoscale). Sources with $25 < D_{2attr.} \leq 100$ (*m* = 26 ÷ 100) can be considered as an outburst of a group of *m* dislocations through an obstacle or their abrupt deceleration by the obstacle. Furthermore, sources with *m* > 100 ($D_{2attr.}$ > 100) shall be viewed as motion of a large condensation, composed from *m* dislocations, or as a simultaneous work of *m* / 100 Frank-Read sources, i.e. as microsources.

Let us consider the AE source distribution dynamics by scale levels depending on the number of previous loading cycles (Fig. 3). Since practically only macrosource signals are recorded during the initial loading of the sample (Fig. 3a,b) under its elastic strain (zone I), alignment of local loading concentrations close to macrodefects and destruction of impurity inclusions takes place. In the course of further loading (Fig. 3c,d) AE microsources become dominant in the sample (zone IV). Dislocation sources start working, bulk movement of disconnected dislocations and their concentration by the boundaries takes place.

During the first loading cycle (Fig. 3e,f) movement of separate dislocations becomes less active and AE mesosources of the second level appear (zone III). A considerable part of dislocations is concentrated in the clusters and does not move freely, but rather breaks through obstacles and stops by the next obstacle. During the repeated loading cycle (Fig. 3g,h) macrosources practically will not be registered, whereas the number of mesosources of the first scale increase (zone II). Dislocation concentration within grains becomes high, and dislocations start reaching the surface. During the

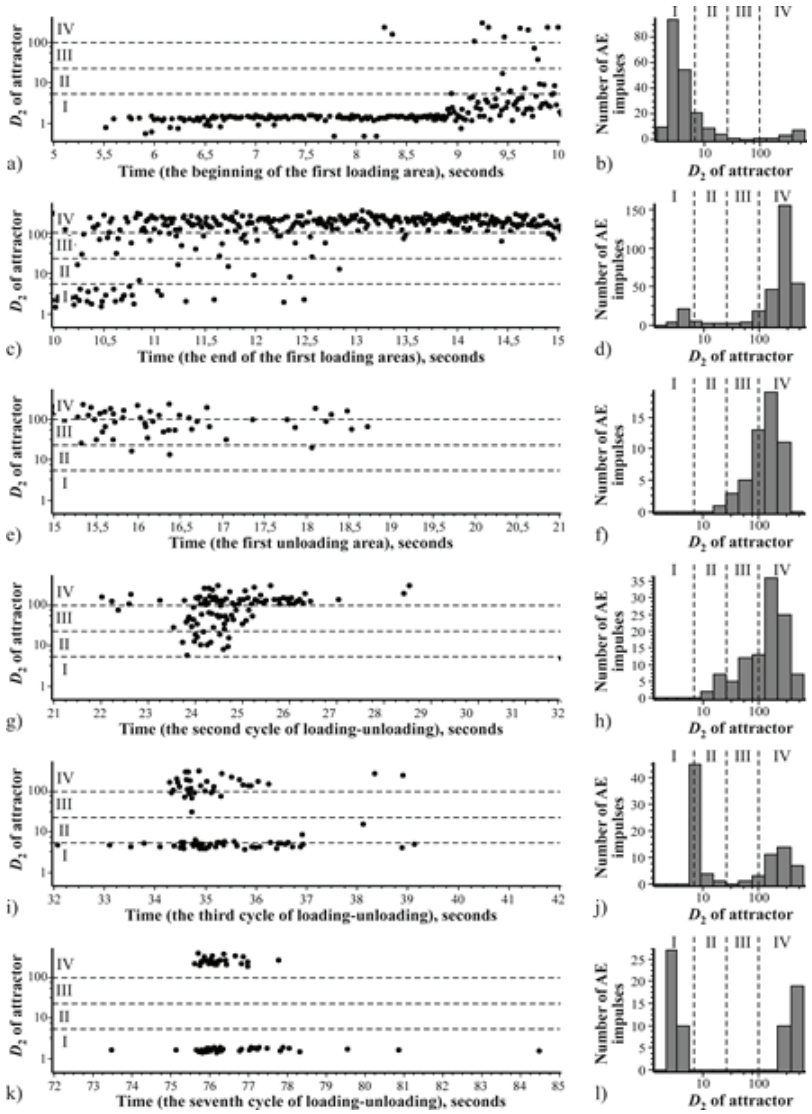

Figure 3: Scale distribution dynamics of AE sources depending on the number of previous loading cycles. Roman numeral denote the following: I – zone of AE macrosources, II – mesosources of the second scale level, III – mesosources of the first scale level, IV – microsources.

third loading cycle (Fig. 3i,j) many mesosources of the second scale level is observed, which apparently testifies that the dislocations are starting to reach the grain surface intensively. This leads to the accumulation of microdefects on the grain boundaries and the formation of cracks. Immediately prior to the reduction of the sample (Fig. 3k,l), the AE signal includes hits, mostly caused by the advancing cracks (macrosources in zone I) and the intense work of dislocation sources (zone IV) in the material areas, which were subjected to non-convertible plastic deformations.

Thus, the possibility to identify the processes, taking place in the loaded sample, by AE fractal analysis was experimentally proved. It can be used to forecast the durability of structures and components.

Let us consider AE characteristics during the first semi-period of the sample loading (Fig. 3a-d). The charts reveal a clear boundary, where the material sample transforms from the elastic to elastoplastic strain. AE hits generated by the microsources ($D_{2attr.}$

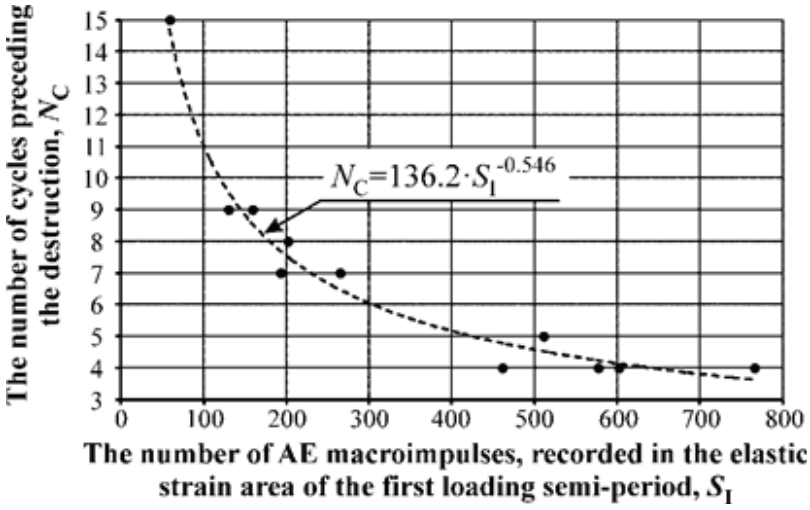

Figure 4: Charts, describing the correlation between the number N_C of loading cycles, preceding the sample destruction, and the number S_I of AE hits with the fractal dimension of the reconstructed attractor $1 \leq D_{2attr.} \leq 6$ (of macro-hits), recorded on the elastic strain area of the first semi-loading period.

≥ 100), are detected in the AE signal at the stage of elastoplastic strain. They are hardly observed at the stage of elastic strain. However, the elastic strain area of the first loading semi-period is characterized by the intense work of AE macrosources, i.e. various structure defects, caused by the imperfection of the sample material, as well as adopted at the manufacturing stage or as a result of wear-out. Thus, the number of the AE hits, recorded in the elastic strain area and identified as a result of work of macrosources ($1 \leq D_{2attr.} \leq 6$), will give grounds to evaluate the concentration of the macrodefects in the analyzed sample material (structures, components), or, in other words, its defect structure and potential durability.

Calculation of AE macro-hits during the first semi-period of fatigue testing of tubular samples showed that this approach is appropriate for the AA2219 aluminum alloy. A regression model, describing the power law between the number N_C of loading cycles, preceding the sample destruction, and the number S_I of macro-hits, recorded in the first semi-period (Fig. 4): $N_C = 136.2 \cdot S_I^{-0.546}$. Determination coefficient for this model is $R^2 = 0.91$, which testifies that the obtained model is of appropriate quality. The model was derived in the course of testing of the 31^{st} sample.

Thus, the regression model allows forecasting durability of products made of AA2219 aluminum alloy based on its AE characteristics during the first loading semi-period. The forecast inaccuracy does not exceed 10%, which is satisfactory for the most technical applications. It is better than all non-destructive durability testing methods known to date.

4. Conclusion

Experimental data presented in this article reveal the multiscale nature of the processes taking place when materials are deformed. Fractal analysis of acoustic emission provides means to detect acoustic emission signals, caused by the deformation

processes of any scale, which are of interest within a given problem, and to accomplish quantitative diagnostics of these processes. The procedures suggested make it possible to use acoustic methods to selectively analyze processes, taking place on the macro-, meso- or micro-levels of the deformed material. These procedures provide means of forecasting the durability of metal samples without their destruction via the selective quantitative analysis of elastic strain macroprocesses.

References

[1] AA. Hlybov, The evaluation of damage accumulation in the construction metal materials by acoustic methods to secure safe operation of technical objects. Nizhny Novgorod, Tech. Rep., 1 AA, Hlybov, 2011.

[2] H. J. Wang and Z. Lin, Detection of fractal characteristics based on acoustic emission, *Materials Science and Technology (United Kingdom)*, **29**, no. 2, 240–249, (2013).

[3] H. L. Dunegan, D. O. Harris, and C. A. Tatro, Fracture analysis by use of acoustic emission, *Engineering Fracture Mechanics*, **1**, no. 1, 105–IN23, (1968).

[4] YuI. Bolotin, BP. Romanov Burov, and Archipov. , Savchenko YuE: On emission detection within the elastic strain limits, 511–514

[5] C. K. Mukhopadhyay, T. Jayakumar, B. Raj, and K. K. Ray, Correlation of acoustic emission with stress intensity factor and plastic zone size for notched tensile specimens of AISI type 304 stainless steel, *Materials Science and Technology*, **18**, no. 10, 1133–1141, (2002).

[6] S. H. Carpenter and F. P. Higgins, SOURCES OF ACOUSTIC EMISSION GENERATED DURING THE PLASTIC DEFORMATION OF 7075 ALUMINUM ALLOY., *Metall Trans A*, **8**, no. 10, 1629–1632, (1977).

[7] VV. Klyuev, Ed., *Non-destructive testing and diagnostics: Reference book*, Mashinostroenie, Moscow, 1995.

[8] A. G. Penkin and V. F. Terent'ev, Acoustic-emission estimation of the damage to 19G structural steel during static and cyclic deformation, *Russian Metallurgy (Metally)*, **2004**, no. 3, 268–273, (2004).

[9] *Cambridge*, Cambridge University Press, Cambridge, 1997.

[10] HDI. Abarbanel, *Analysis of observed chaotic data*, Springer, New York, 1996.

[11] P. Grassberger and I. Procaccia, Characterization of strange attractors, *Physical Review Letters*, **50**, no. 5, 346–349, (1983).

[12] F. Takens, *Detecting strange attractors in turbulence. Lect not math*, 12 F, Takens, 1981.

[13] OE. Sysoev, EA. Kuznetsov, and Kurinyi. , Shport RV: Modern testing equipment for analysing construction materials under low-cycle strains and combined tension with acoustic emission parameters taken into account. Memoirs KASTU, in *Kurinyi VV*, **9**, 106–112, 9(1, 2012.

[14] R. Hegger, H. Kantz, and T. Schreiber, Practical implementation of nonlinear time series methods: The TISEAN package, *Chaos*, **9**, no. 2, 413–435, (1999).

[15] R. Hegger, H. Kantz, and T. Schreiber, *TISEAN 3.0.1. Nonlinear Time Series Analysis*, 2007, http://www.mpipks-dresden.mpg.de/.

[16] A. Mekler, Calculation of EEG correlation dimension: Large massifs of experimental data, *Computer Methods and Programs in Biomedicine*, **92**, no. 1, 154–160, (2008).

[17] OE. Sysoev, Bilenko SV: Forecasting long-term strength-based construction materials fractal analysis of acoustic emission, in *Memoirs KASTU*, **11**, 107–115, 11(1, 2012.